G. R. Liu
K. Y. Lam
Department of Mechanical and Production Engineering
National University of Singapore
10 Kent Ridge Crescent, S0511
Singapore

E. S. Chan
Department of Civil Engineering
National University of Singapore
10 Kent Ridge Crescent, S0511
Singapore

Stress Waves in Composite Laminates Excited by Transverse Plane Shock Waves

A simple 1-dimensional model is presented to investigate elastic stress waves in composite laminates excited by underwater explosion shocks. The focus is on the elastic dynamic stress fields in the composite laminate immediately after the action of the shock wave. In this model, the interaction between the laminate and the water is taken into account, and the effects of the laminate–water interaction on the stress wave fields in the laminate are investigated. In the formulation of the model, wave fields in the laminate and the water are the first obtained in the frequency domain and then transferred into the time domain using the Fourier transform techniques. A quadrature technique is used to deal with the Fourier transform integrals in which the integrands have very sharp peaks on the integral axis. Numerical examples for stress waves in a steel plate and a glass reinforced plastic sandwich laminate are presented. The technique and the results presented in this article may be used in the design of ship hull structures subjected to underwater explosions. © *1996 John Wiley & Sons, Inc.*

INTRODUCTION

Composites, such as glass-fiber reinforced plastic (GRP) and sandwich structures, are ideal materials for the hull and superstructure of marine vessels. This is largely due to the high ratio of strength and stiffness to weight, ease of fabrication, and the resistance to corrosion. For naval vessels such as mine countermeasures vessels (MCMV), GRP composites have the additional advantage of being nonmagnetic and hence have a higher protection against magnetic mines. For these reasons GRPs have been used to build a large number of naval vessels (Trimming, 1978; Hall and Robson, 1984; Hall, 1989). However, naval vessels could still be subjected to underwater explosions and the resulting shock waves may cause severe structural damage. Detailed investigations on the responses of GRP to the underwater shock loading are therefore very important, particularly in understanding the mechanism of shock damage.

In the 1980s a number of important experimental studies were conducted to investigate the behavior of sandwich structures subjected to underwater explosion. Green (1982), Hall and Robson (1984), and Hall (1989) examined the resistance of GRP–foam sandwich panels to underwater blast

Received May 9, 1995; Accepted May 16, 1996.

Shock and Vibration, Vol. 3, No. 6, pp. 419–433 (1996)

CCC 1070-9622/96/060419-15

damage. In their experiments, samples of the sandwich panels were subjected to different levels of underwater explosions. Different types of damage within the foam material and delamination at the GRP–foam interfaces were observed. A small scale experimental study of shock damage in GRP laminates was also conducted by Mouritz et al. (1993). In these tests, damage in the matrix of the GRP laminates was observed and the effects of air and water backing on the rearward side of the GRP laminates were examined. The residual tensile fracture strength of the laminates after being exposed to the underwater blast was also measured.

The response of a composite laminated plate subjected to an underwater shock loading is, in general, rather complex. The failure in the matrix or the delamination in the interface of the layers is naturally dependent on how the stress waves propagate in the laminates. Therefore, to have a better understanding of the failure or the mechanism of the delamination or damage when subjected to a shock loading, a detailed dynamic stress analysis would be necessary.

In this article, a simple 1-dimensional model is presented to investigate elastic stress waves in composite laminates excited by shock waves due to underwater explosions. The focus of this study is on the elastic dynamic displacement and stress fields in an air-backed composite laminate at the early stages of the shock action. In this model, the interaction between the laminate and the water is taken into account and the effects of the laminate–water interaction on the wave fields in the laminate are also investigated. For simplicity, the initial shock pressure is prescribed using an empirical formula. It is assumed that the water is acoustical and that there is no cavitation in the water. In the formulation of the model, wave fields in the laminate and the water are first obtained in the frequency domain. Stress waves in the laminate are then obtained in the time domain using the Fourier transform (FT) techniques. A quadrature technique is used in the evaluation the FT integrals, in which the integrands have very sharp peaks on the integral axis. Numerical examples for stress waves in a steel plate and a GRP sandwich laminate excited by underwater explosions are presented. Stress fields are computed and discussed in detail. The technique and the results presented here may be used in the design of ship hull structures subjected to underwater explosions.

FORMULATION

Figure 1 shows the schematic drawing of a laminate subjected to an underwater explosion. The explosive charge is placed in the water on the right-hand side of the laminate with a standoff distance of D. The left surface of the laminate is

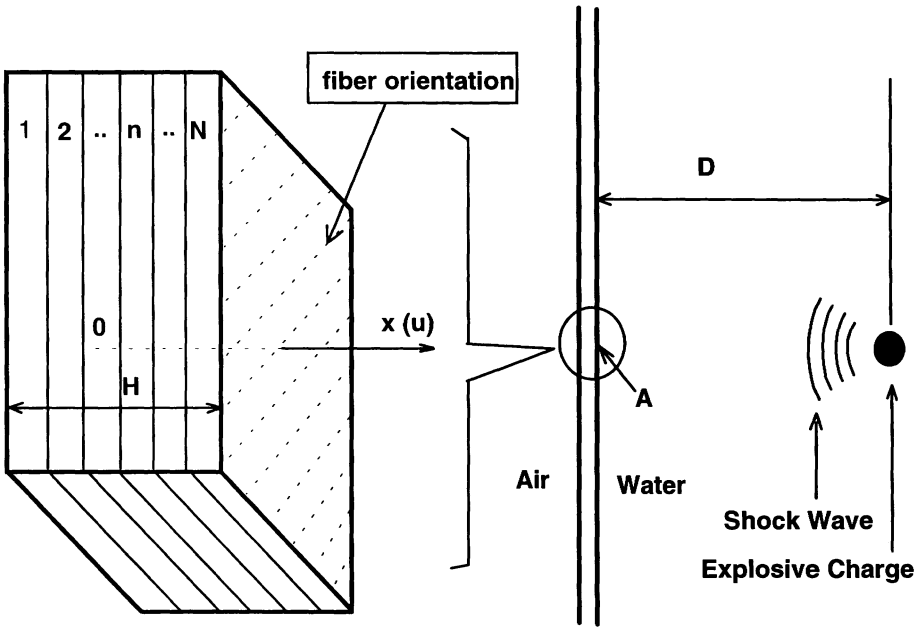

FIGURE 1 An isotropic laminate subjected to an underwater explosion.

backed with air. For generality, we consider a laminate consisting of an arbitrary number of fiber reinforced layers. The fibers are laid in the laminate plane. The thickness of the laminate and the nth layer is denoted, respectively, by H and h_n. It is assumed that the standoff distance D is much larger then the plate thickness H and we are only interested in a very small region near point A, the first contact point of the shock wave. The shock wave can therefore be treated as a plane wave and the problem is treated as 1-dimensional. The objective of this article is to examine the elastic waves in the laminate subjected to underwater shock waves. To simplify the problem, and to concentrate on the wave fields in the laminates and the laminate–water interaction, the problem is solved using the following procedure. In the absence of the laminate, the pressure in the water is first obtained by an empirical formula for underwater explosion. The pressure generated by the shock wave is then considered as an incident plane wave to the laminate–water interaction system. This system is then analyzed to yield the displacement and stress fields in the laminate.

Pressure Caused by Shock Wave

The pressure at point A due to an underwater explosion is derived from the empirical equation (Geers and Shin, 1994),

$$P(t) = \begin{cases} P_{\max} e^{-(t/t_d)}, & t > 0 \\ 0 & t \le 0 \end{cases}, \tag{1}$$

where t is the time measured from the arrival of the shock wave at point A (see Fig. 1). In Eq. (1) $P_{\max}$ is the peak pressure of the shock wave, and t_d is a decay constant pertaining to the exponential decay. The peak pressure is given by

$$P_{\max} = C_1 \left(\frac{W^{1/3}}{D} \right)^{C_2}, \tag{2}$$

and the time decay constant is obtained by

$$t_d = C_3 W^{1/3} \left(\frac{W^{1/3}}{D} \right)^{C_4}. \tag{3}$$

In Eqs. (2) and (3) W is the weight of the explosive charge and C_i ($i = 1, \ldots, 4$) are constants depending on the explosive type. For TNT, the explosive considered in this study, $C_1 = 52.116$, $C_2 = 1.18$, $C_3 = 0.08957$, and $C_4 = -0.185$. In Eqs. (2) and (3), the distance is in meters, the time is in milliseconds, the weight is in kilograms, and the pressure is in mega Pascals.

Figure 2 shows the pressure $P(t)$ at point A. The standoff distance is 10 m, and the charge is 20 kg TNT. The peak pressure at point A is 11.187 MPa. From Fig. 2 it is seen that the distribution of the pressure on the laminate surface decays exponentially with respect to time.

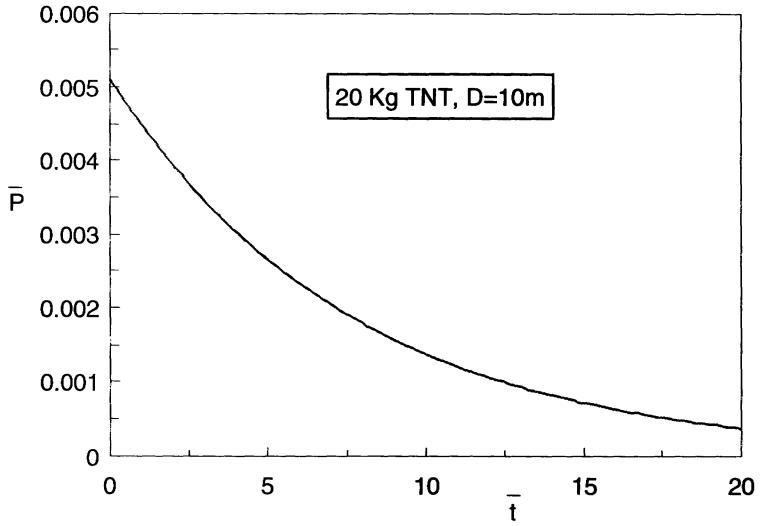

FIGURE 2 Pressure in the water produced by an underwater explosion in the absence of the laminate.

Simple Model for Laminate–Water Interaction System

A simple model is used for the simulation of the elastic wave fields excited by an underwater explosion. In this model, wave fields in the laminate and the water are obtained in the frequency domain. The interaction of the laminate and water is taken into account using the continuity conditions between the laminate and the water. The wave field in the time domain is then obtained using FT techniques.

The global coordinate system for the whole laminate–water system is shown in Fig. 1. In the following formulation, local coordinate systems are used for each layer of the laminate and the water. The origin of the local coordinate system is at the left surface of each layer or the water, and the orientation of each local coordinate system coincides with the global coordinate system.

Wave Field in Frequency Domain.

Wave Field in Laminate. For a layer of the laminate, the system of governing differential equations (in the absence of body force) is expressed as

$$\rho \frac{\partial^2 u}{\partial t^2} - c_{11} \frac{\partial^2 u}{\partial x^2} = 0, \tag{4}$$

where ρ is the mass density, c_{11} is the elastic constant of the material, and u is the displacement in the x direction. Because a plane wave is considered here, the only nonzero strain component in the layer is ε_{xx}.

$$\varepsilon_{xx} = \frac{\partial u}{\partial x}, \tag{5}$$

and the nonzero stress components are given by

$$\sigma_{xx} = c_{11}\varepsilon_{xx}, \quad \sigma_{yy} = c_{12}\varepsilon_{xx}, \quad \sigma_{zz} = c_{13}\varepsilon_{xx}. \tag{6}$$

It is seen from Eq. (6) that the difference between the stress components is the coefficient of the material constants. Therefore, only σ_{xx} needs to be discussed and is noted by σ hereafter. Other stress components can be obtained easily just by multiplying a factor. It is assumed that the displacement in the frequency domain has the form of

$$u = d\exp(i\xi x)\exp(i\omega t), \tag{7}$$

where d is the amplitude of the displacement, ξ is the wave number in the x direction, and ω is the angular frequency. Substituting Eq. (7) into (4), we obtain

$$(\rho\omega^2 - \xi^2 c_{11})d = 0. \tag{8}$$

The satisfaction of Eq. (8) requires the term within the brackets to be set to zero. Hence, we obtain

$$\xi = \pm k = \pm\sqrt{\frac{\rho}{c_{11}}}\,\omega. \tag{9}$$

The general solution for Eq. (4) can then be expressed by

$$u = U\exp(i\omega t), \tag{10}$$

where U is the amplitude of the displacement in the frequency domain given by

$$U = A^+\exp(ikx) + A^-\exp(-ikx), \tag{11}$$

where A^+ and A^- are constants. It can be seen from Eqs. (10) and (11) that the first term on the right-hand side of Eq. (11) represents waves propagating in the negative x direction and the second term represents the waves propagating in the positive x direction.

Equations (5), (6), (10), and (11) yield

$$\sigma = S\exp(i\omega t), \tag{12}$$

where S is the amplitude of the stress in the frequency domain given by

$$S = ikc_{11}[A^+\exp(ikx) - A^-\exp(-ikx)]. \tag{13}$$

Equations (10) and (12) are the solutions for all the N layers in the laminate. Therefore $2N$ constants are needed to be determined by the boundary conditions for the laminate and continuity conditions on the interfaces of the layers and the interface between the laminate and the water.

Wave Field in Water. For a wave field in the water, we assume that the water is acoustic; namely, the movement of particles in the water is very small. This assumption is valid when the explosion is far from the plate surface. For an acoustic water without sources, the governing differential equations can be expressed by

$$\frac{\partial^2\phi}{\partial t^2} - c_w^2 \frac{\partial^2\phi}{\partial x^2} = 0, \tag{14}$$

where c_w is the wave velocity in the water and ϕ is the velocity potential. The pressure p and velocity v in the water can be obtained, respectively, by

$$p = \rho_w \frac{\partial\phi}{\partial t}, \tag{15}$$

$$v = -\frac{\partial\phi}{\partial x}. \tag{16}$$

Cmparing Eq. (14) with (4), the general solution for Eq. (14) can be immediately written as

$$\phi = [A_w^+ \exp(ik_w x) + A_w^- \exp(-ik_w x)]\exp(i\omega t). \tag{17}$$

where

$$k_w = \frac{\omega}{c_w}. \tag{18}$$

In Eq. (17), A_w^+ and A_w^- are constants. The first term on the right-hand side of Eq. (17) represents waves propagating in the negative x direction and the second term represents the waves propagating in the positive x direction.

Interaction Between Laminate and Water. For generality, we first assume that the laminate is loaded on the two surfaces and the $(N-1)$ interfaces. Hence, the external force vector can be written as

$$\mathrm{T} = \{T_1 \quad T_2 \quad \cdots \quad T_N \quad T_{N+1}\}, \tag{19}$$

where T_j is the external force acting on the jth interface, $j = 1$ is for the left surface, and $j = N + 1$ is for the right surface of the laminate. The boundary condition for the laminate can be written as follows for the left surface of the laminate,

$$-\sigma_1^{\mathrm{L}} = T_1. \tag{20}$$

For the interfaces in the laminate,

$$\sigma_n^{\mathrm{R}} - \sigma_{n+1}^{\mathrm{L}} = T_{n+1}, \quad u_n^{\mathrm{R}} = u_{n+1}^{\mathrm{L}}, \quad \text{for } 1 \le n \le (N-1). \tag{21}$$

In Eqs. (20) and (21) the subscripts for σ and T denote the layer numbers, and the superscripts R and L stand, respectively, for the right and left surfaces of a layer.

Considering the boundary conditions in the water, it is noted that, in the positive x direction, the water goes to infinity. The radiation condition, which states that waves are left-going toward infinity, must therefore be satisfied. Consequently, the first term on the right-hand side of Eq. (17) must vanish and the velocity potential in the water can be rewritten as

$$\phi = A_w^- \exp(-ik_w x)\exp(i\omega t). \tag{22}$$

Substituting Eq. (22) in Eqs. (15) and (16), the pressure and velocity in the water can be obtained by

$$p = A_w^- i\omega\rho_w \exp(-ik_w x)\exp(i\omega t), \tag{23}$$

and

$$v = A_w^- \, i\frac{\omega}{c_w} \exp(-ik_w x)\exp(i\omega t). \tag{24}$$

On the interface between the laminate and the water, the following continuity equations are satisfied:

$$\sigma_N^{\mathrm{R}} + p|_{x=0} = T_{N+1} - p^{\mathrm{in}}|_{x=0}, \tag{25}$$

where p^{in} is the pressure on the plate surface caused by the incident plane shock wave, and

$$v_{x=0}^{\mathrm{in}} + v_{x=0} = \frac{\partial u_N^{\mathrm{R}}}{\partial t} = i\omega u_N^{\mathrm{R}}, \tag{26}$$

where $v_{x=0}^{\mathrm{in}}$ is the velocity on the plate surface caused by the incident plane shock wave. It can be easily found from Eqs. (15) to (17) that $v_{x=0}^{\mathrm{in}} = -p^{\mathrm{in}}/(c_w\rho_w)$. It may be noted that for the incident wave, the second term on the right-hand side of Eq. (17) must vanish.

Substitution of Eqs. (10), (12), (23), and (24) into Eqs. (25) and (26), leads to

$$T_{N+1} - p^{\mathrm{in}}|_{x=0} = e_{sN}^+ A_N^+ - e_{sN}^- A_N^- + i\rho_w\omega A_w, \tag{27}$$

and

$$-p^{\mathrm{in}}|_{x=0} = i\rho_w\omega c_w e_{uN}^+ A_N^+ + i\rho_w\omega c_w e_{uN} A_N - i\rho_w\omega A_w^-, \tag{28}$$

where

$$e_{un}^{+} = \exp(ik_n h_n), \quad e_{un}^{-} = \exp(-ik_n h_n), \quad (29)$$

and

$$\begin{aligned} e_{sn}^{+} &= ik_n c_{11(n)} \exp(ik_n h_n), \\ e_{sn}^{-} &= ik_n c_{11(n)} \exp(-ik_n h_n). \end{aligned} \quad (30)$$

The subscript $n(=1, 2, \ldots, N)$ denotes the layer number. Eliminating A_w^- from Eqs. (27) and (28) yields

$$\begin{aligned} T_{N+1} - 2p^{in} = (e_{sN}^{+} + i\rho_w c_w \omega e_N^{+}) A_N^{+} \\ + (-e_{sN}^{-} + i\rho_w c_w \omega e_{uN}^{-}) A_N^{-}. \end{aligned} \quad (31)$$

Assembling Eqs. (20), (21), and (29), we obtain the following equation for the whole laminate–water interaction system.

$$\mathrm{F} = \mathrm{KA}, \quad (32)$$

where F is the total external force vector contributed from the external force T and the incident wave pressure. Vector F can be obtained from T by replace T_{N+1} in T by $(T_{N+1} - 2p^{in})$. In Eq. (32) A is a consistent vector for all the layers

$$\mathrm{A} = \{A_1^{+} \quad A_1^{-} \quad A_2^{+} \quad A_2^{-} \quad \cdots \quad A_N^{+} \quad A_N^{-}, \quad (33)$$

and the matrix K is given by

$$\mathrm{K} = \begin{bmatrix} k_{E1} & k_{E1} & 0 & 0 & 0 & 0 & 0 & \cdots & 0 \\ e_{u1}^{+} & e_{u1}^{-} & -1 & -1 & 0 & 0 & 0 & \cdots & 0 \\ e_{s1}^{+} & e_{s1}^{-} & -k_{E2} & k_{E2} & 0 & 0 & 0 & \cdots & 0 \\ 0 & 0 & e_{u2}^{+} & e_{u2}^{-} & -1 & -1 & 0 & \cdots & 0 \\ 0 & 0 & e_{s2}^{+} & -e_{s2}^{-} & -k_{E3} & k_{E3} & 0 & \cdots & 0 \\ \vdots & \vdots & \cdots & \ddots & \ddots & \ddots & \vdots & \cdots & \vdots \\ 0 & 0 & \cdots & 0 & 0 & 0 & 0 & (e_{sN}^{+} + ir_w e_{uN}^{+}) & (-e_{sN}^{-} + ir_w e_{uN}^{-}) \end{bmatrix}, \quad (34)$$

where

$$k_{En} = ik_n c_{11(n)}, \quad n = 1, 2, \ldots, N, \quad (35)$$

$$r_w = \rho_w c_w \omega. \quad (36)$$

Solving Eq. (32), the constant vector A can be obtained, and the displacement and stress in each layer can be obtained by Eqs. (10) and (12).

Wave Field in Time Domain

Fourier Transform Technique. Once the displacement in the frequency domain is known, the displacement in the time domain can be obtained by the Fourier superposition

$$u_t(t) = \frac{1}{2\pi} \int_{-\infty}^{\infty} U(\omega) \tilde{P}(\omega) \exp(i\omega t) d\omega, \quad (37)$$

where $\tilde{P}(\omega)$ is the FT of the external load and is given by

$$\tilde{P}(\omega) = \int_0^{\infty} P(t) \exp(-i\omega t) dt. \quad (38)$$

From Eq. (38) it is easily understood that

$$\tilde{P}(-\omega) = \tilde{P}^*(\omega), \quad (39)$$

where the asterisk denotes the complex conjugate. From Eqs. (4)–(36) it is also found that

$$U(-\omega) = U^*(\omega). \quad (40)$$

With the help of Eqs. (39) and (40), Eq. (37) can be reduced to

$$\begin{aligned} u_t(t) = \frac{1}{\pi} \Bigg[\int_0^{\infty} (U_R \tilde{P}_R - U_I \tilde{P}_I) \cos \omega t d\omega \\ - \int_0^{\infty} (U_R \tilde{P}_I - U_I \tilde{P}_R) \sin \omega t d\omega \Bigg], \end{aligned} \quad (41)$$

where U_R and U_I are, respectively, the real and imaginary parts of U, and $\tilde{P}_R$ and $\tilde{P}_I$ are, respectively, the real and imaginary parts of $\tilde{P}$.

The stress in the time domain can be obtained in exactly the same way as the displacement:

$$\sigma_t(t) = \frac{1}{\pi}\left[\int_0^\infty (S_R\tilde{P}_R - S_I\tilde{P}_I)\cos \omega t d\omega - \int_0^\infty (S_R\tilde{P}_I - S_I\tilde{P}_R)\sin \omega t d\omega\right], \tag{42}$$

where S_R and S_I are, respectively, the real and imaginary parts of stress S given by Eq. (13).

Technique for Evaluation of Fourier Integral. The integral in Eqs. (41) and (42) can be evaluated by ordinary routines using equally spaced sampling points. However, the sampling points can be very large because S_R and S_I (or U_R and U_I) vary very rapidly near the singular points of the matrix K given in Eq. (34) where $r_w = 0$. Figure 3 shows an example of the rapidly varying S_R and S_I. It is also not easy to control the accuracy of integration using equally spaced routines. To minimize the sampling points and yet achieve accuracy of the integration, an adaptive scheme suggested by Liu et al. (1995) was employed to evaluate integrals in Eqs. (41) and (42). A brief of the adaptive scheme is given as follows.

Consider a general case of a sine Fourier integral,

$$\tilde{G}(t) = \frac{1}{\pi}\int_a^b G(\omega)\sin \omega t d\omega, \tag{43}$$

where $G(\omega)$ varies very rapidly at some points on the ω axis. In this scheme $G(\omega)$ is represented by piecewise second-order polynomials and the Fourier integration is carried out exactly for each piece. The key point in this scheme is to compute the piecewise polynomials and make the procedure adaptive. In the integration region $[a, b]$, $d = (b - a)/(4m)$, where m is any integer, can be used as a primary increment in computing $G(\omega)$. Initially, we calculate $G(a)$. On the first step we compute four increments and obtain $G(a + d)$, $G(a + 2d)$, $G(a + 3d)$, and $G(a + 4d)$. Next, by using the three points $G(a)$, $G(a + 2d)$, and $G(a + 4d)$, a second-order polynomial, $g(k)$, can be formed, and $g(a + d)$ and $g(a + 3d)$ can be obtained,

$$g(a + d) = 0.125[3G(a) + 6G(a + 2d) - G(a + 4d)], \tag{44}$$

$$g(a + 3d) = 0.125[-G(a) + 6G(a + 2d) + 3G(a + 4d)]. \tag{45}$$

Next, we check

$$\left|\frac{G(a + d) - g(a + d)}{G(a + d)}\right| \le \tau, \tag{46}$$

and

$$\left|\frac{G(a + 2d) - g(a + 2d)}{G(a + 2d)}\right| \le \tau, \tag{46}$$

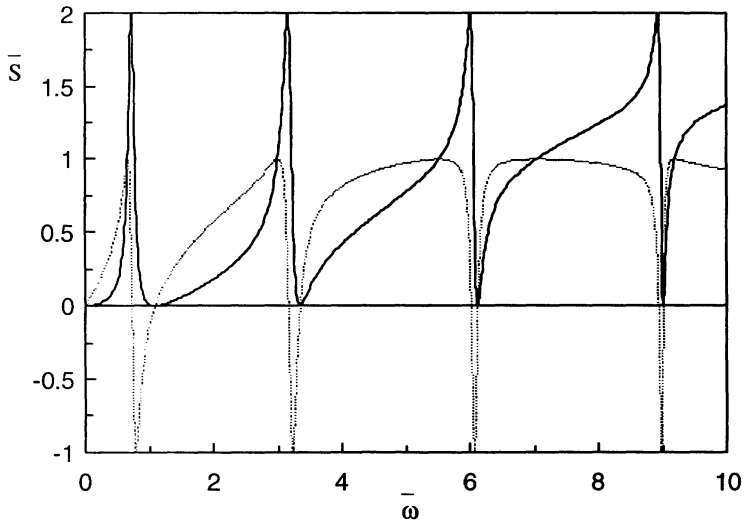

FIGURE 3 Stress in the frequency domain: sandwich plate, $x = H$, (——) real part, (···) imaginary part.

where τ is the tolerance. If Eqs. (46) and (47) are satisfied, we go to the next four steps until reaching b. If one of Eqs. (46) and (47) is not satisfied, d is halved and we go back to the first step. In this case only $G(a + d/2)$, $G(a + 3d/2)$, $G(a + 5d/2)$, and $G(a + 7d/2)$ need to be computed, and the previously computed Gs and ωs can be saved and kept in order for later uses. Finally, the integration region $[a, b]$ is divided into M pieces, and $2M + 1$ Gs and ωs are obtained. The integral in Eq. (43) can be written as

$$\int_a^b G(\omega)\sin \omega t d\omega \approx \sum_{j=1}^{M} \int_{\omega_j}^{\omega_{j+2}} g(\omega)\sin \omega t d\omega, \quad (48)$$

where

$$g(\omega) = \left[\left(1 - 3\frac{\omega}{d} + 2\frac{\omega}{d^2}\right) \quad 4\left(\frac{\omega}{d} - \frac{\omega^2}{d^2}\right) \quad \left(-\frac{\omega}{d} + 2\frac{\omega^2}{d^2}\right)\right] \begin{Bmatrix} G_j \\ G_{j+1} \\ G_{j+2} \end{Bmatrix}, \quad (49)$$

where $d = \omega_{j+2} - \omega_j$ and $G_j = G(\omega_j)$. Obviously, integrations on the right-hand side of Eq. (48) can be easily carried out analytically.

For the cosine Fourier integral, a similar technique is applicable.

NUMERICAL EXAMPLES

A program was made in FORTRAN-77 to compute the wave field in the laminates subjected to underwater explosions. Two plates, an isotropic and homogeneous steel plate and a sandwich laminate consisting of one core layer and two face layers of equal thickness, were investigated. The material constants are given in Table 1. For the convenience of comparison, the thickness of the steel plate is set to 60 mm, the same as the sandwich plate. This is, of course, very thick for a steel plate. As will be seen later, dimensionless parameters are used in this study. Hence, the results for the steel plate can be used for any thickness.

Table 1. Dimensions and Material Parameters for Steel Plate and Sandwich Laminate

	Thickness (mm)	E (N/m^2)	ρ (kg/m^3)	ν
Steel	60	7.74E10	7900	0.3
Two face layers	5	1.67E10	1760	0.3
Core layer	50	0.013E	130	0.3

The term wet laminate used here means that the laminate–water interaction in the right surface of the laminate is taken into account by the method described earlier. The present technique can also be easily used for dry laminate for which the laminate–water interaction in the right surface of the laminate is ignored, and the laminate is simply loaded by two times the pressure given by Eq. (1). All the equations for the laminate given are valid for the dry laminate if we set $r_w = 0$ in Eq. (34). However, caution has to be taken when evaluating the integrals in Eqs. (41) and (42). This is because the integrands have singularity points on the integral axis if the materials of the laminate are pure elastic. Therefore, the integrals in Eqs. (41) and (42) for the dry laminate should be evaluated by the so-called exponential window method (see e.g., Liu and Achenbach, 1995). Both dry and wet laminates were investigated and are discussed in this section.

In the computation, the following dimensionless parameters are used.

$$\bar{u} = u/H, \quad \bar{\rho} = \rho/\rho_w, \quad \bar{P} = P/E_w, \quad \bar{\sigma} = \sigma/E_w, \quad \bar{c}_{11} = c_{11}/E_w, \quad \bar{\omega} = \omega H/c_w, \quad \bar{t} = tc_w/H, \quad (50)$$

where $E_w = c_2^2\rho_w$, and $\bar{t} = 1$ is the real time for the shock wave traveling a distance of H once.

If the external force T given by Eq. (19) is zero, the total external force vector F is contributed only by the incident shock wave generated by the explosion,

$$F = \{0 \quad 0 \quad 0 \quad \cdots \quad 0 \quad 0 \quad 2P\}, \quad (51)$$

where P is the pressure of the shock wave given by Eq. (1). It is noted that for convenience, the pressure is treated as a positive force on the laminate–water interaction system. Hence, the computed positive stresses are actually compressive stresses, and the computed negative stresses represent tensile stresses.

The results obtained by the present program were confirmed by checking the satisfaction of the boundary conditions [Eqs. (20), (21), (25), and (26)] after obtaining the displacement and stress field in the laminate. A 1-dimensional finite element model for the steel plate was also built, and MSC/NASTRAN-USA code was used for the

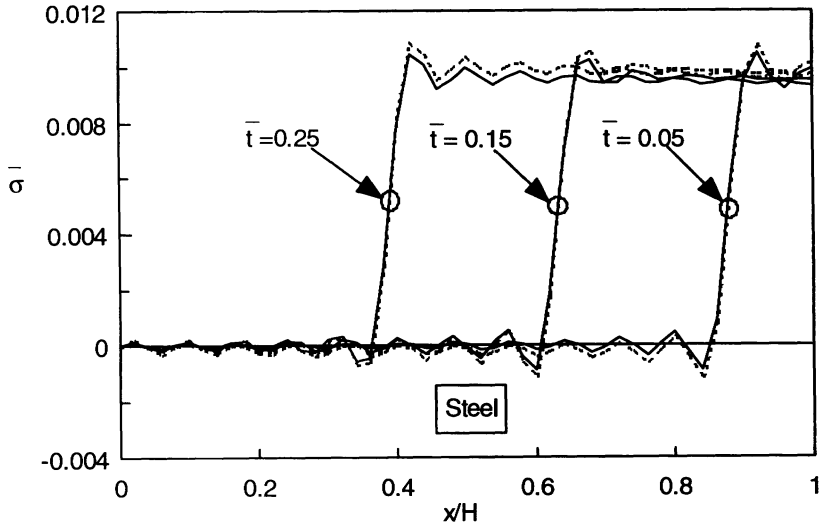

FIGURE 4 Stress distribution in the steel plate subjected to an underwater explosion: (——) wet plate, (···) dry plate; TNT, 20 kg, D = 10 m.

analysis. The results agree well with the results by the present method (data not shown).

Results for Steel Plate

Figure 4 shows the stress distribution in the steel plate at $\bar{t}$ = 0.05, 0.15, and 0.25. The solid lines are for the wet plate and the dotted lines are for the dry plate. It can be seen from this figure that there are small oscillations on the curves. This may be attributed to the error in the evaluation of the Fourier integral given in Eqs. (41) and (42). In these integrals, the integration should have been carried out over zero to infinity. In practice, however, the integration has to be truncated to a finite range. The truncation error appears as small oscillations on the stress distribution curves. We also confirmed that with less truncation, the oscillations are smaller.

Figure 4 shows the compressive stress wave generated by the shock wave propagating leftward. Because a 1-dimensional wave is discussed here, the wave is nondispersive; and the amplitude of the stress wave does not change during its propagation within the plate. The speed of the stress wave is $c_i = \sqrt{c_{11}/\rho}$. From Fig. 4 it can also be seen that, at this stage, there are no significant differences between the results for the dry and wet plates. As time passes (Fig. 5), significant differences between the results for the dry and wet plate can be observed. In addition, a tensile stress is also evident in Fig. 5. The cause for the tensile stress is discussed as follows.

Figure 6 shows the time history of the stress in the steel dry plate at x = 0, 0.2H, 0.9H, and H. Because x = 0 is the left free surface of the plate, the stress is zero. On the right surface ($x = H$), which faces the shock wave, the plate experiences a compressive stress of the same magnitude as the shock pressure obtained by Eq. (1). The compressive stress propagates leftward. At any point inside the plate, say x = 0.2H, the left-going compressive stress wave arrives after a finite time, which is consistent with expectation. The left-going compressive stress wave hits the left free surface of the plate and is reflected back as a right-going tensile wave. After the reflection, the right-going tensile stress wave combines with the left-going compressive wave to result in a smaller tensile stress. For the dry plate, the amplitude of the stress wave does not change when it is propagating in the plate. However, the pressure generated by the shock wave decays exponentially with respect to time (cf. Fig. 2). Therefore, the amplitude of the tensile stress wave reflected from the left surface of the plate is always greater than that of the compressive stress wave generated by the shock pressure. Hence, the combination of the tensile stress wave and the compressive wave results in a small tensile wave. This small tensile wave hits the right surface of the plate and changes back to a compressive wave. As a result, a point in the plate will experience

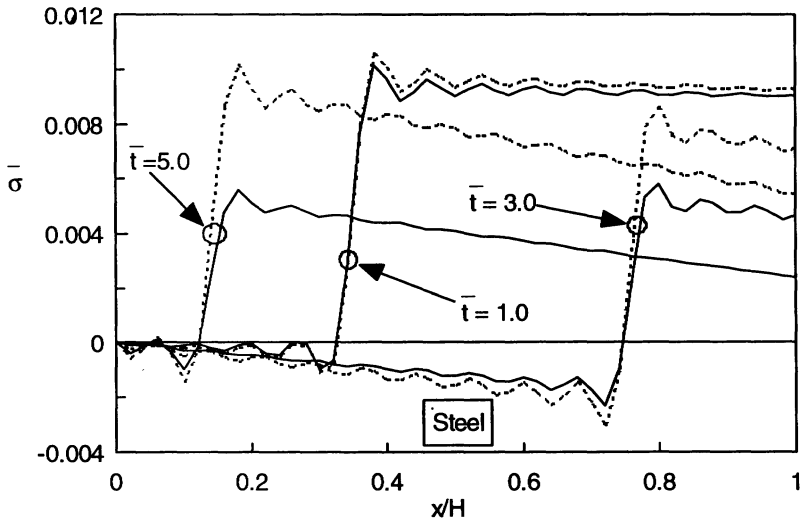

FIGURE 5 As in Fig. 4, but for $\bar{t}$ = 1.0, 3.0, and 5.0.

oscillatory compressive and tensile stresses. The biggest tensile stress is observed at a point nearest (but not equal) to the right surface of the plate. From Fig. 5 a tensile stress of about $0.4P_{max}$ can be found at $x = 0.9H$. Theoretically, the tensile stress could be as big as P_{max} at a point nearest (but not equal) to the right surface of the plate, when the pressure on the right surface of the plate decays to zero.

Figure 7 shows the time history of the stress in the wet plate of steel at $x = 0$, $0.2H$, $0.9H$, and H. Because the plate–water interaction is taken into account, the energy is continuously leaking to the water. Hence, the amplitudes of the compressive and tensile stress waves are gradually reduced. The biggest compressive stress, $2P_{max}$ can be observed at $x = H$, and the biggest tensile stress can be found at the point nearest to $x = H$. For $x = 0.9H$, it was found that the tensile stress is about $0.65P_{max}$. Therefore, if the material is weak in tension, this tensile stress could cause damage near the wet surface, even though it can withstand the compressive stress of the pressure of the shock wave. For a GRP plate, delamination could occur due to the tensile stress.

From Figs. 4 and 5 it can be seen that the

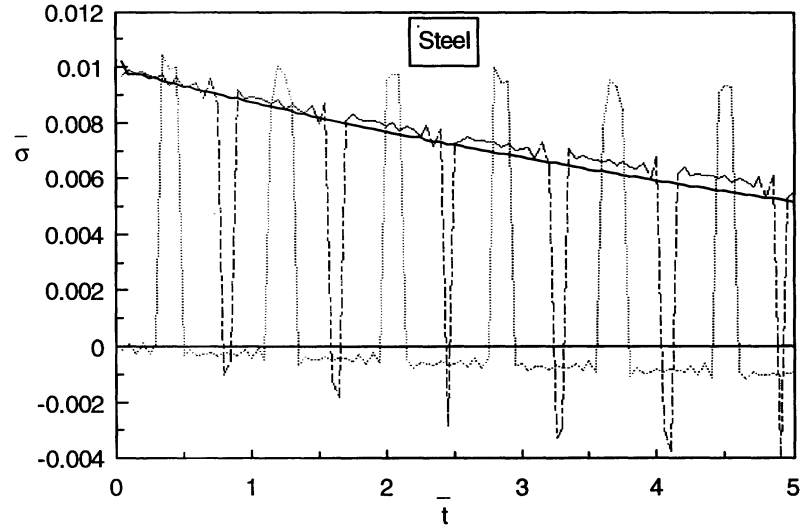

FIGURE 6 Stress history for the steel dry plate subjected to an underwater explosion: (——) $x = H$, (···) $x = 0.2H$, (---) $x = 0.9H$; TNT, 20 kg, D = 10 m).

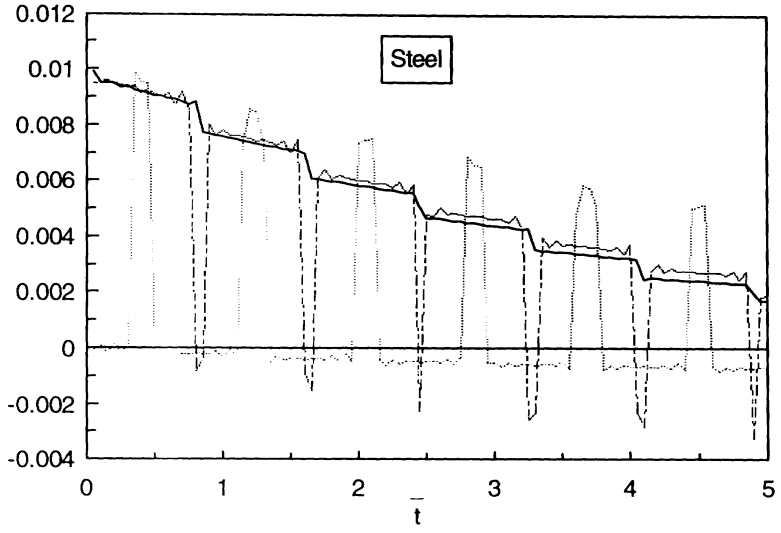

FIGURE 7 As in Fig. 6, but for steel wet plate.

magnitudes of the compressive and tensile stress in the dry plate is greater than that in the wet plate. Therefore, a design is on the conservative side if the stresses are obtained by ignoring the plate–water interaction.

Results for Sandwich Laminate

Figure 8 shows the stress distribution in the sandwich laminate at $\bar{t} = 0.05, 0.15$, and 0.25. Because the stress is zero in the region of $0 \leq x \leq 0.7H$, Fig. 8 shows the stress only in the region of $0.7H \leq x \leq H$. The solid lines are for the wet plate and the dotted lines are for the dry plate. From Fig. 8 it can be seen that there are significant differences between the results for the dry and wet laminate. As time passes (Fig. 9) more significant differences between the results for the dry and wet plate can be observed. From Fig. 8 tensile stresses are also observed. The tensile stress, however, is much smaller than that observed for the single layer plate. The reason may be given as follows.

The sandwich laminate consists of three layers,

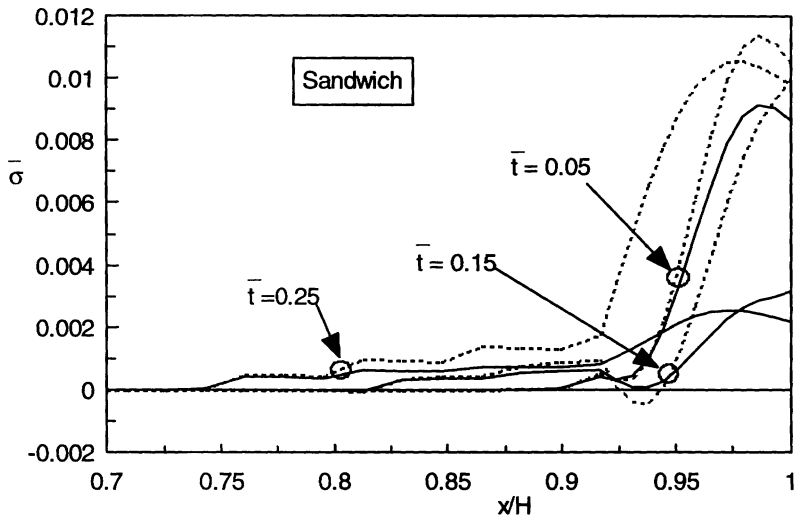

FIGURE 8 Stress distribution in the sandwich laminate subjected to an underwater explosion: (——) wet laminate, (···) dry laminate; TNT, 20 kg, D = 10 m).

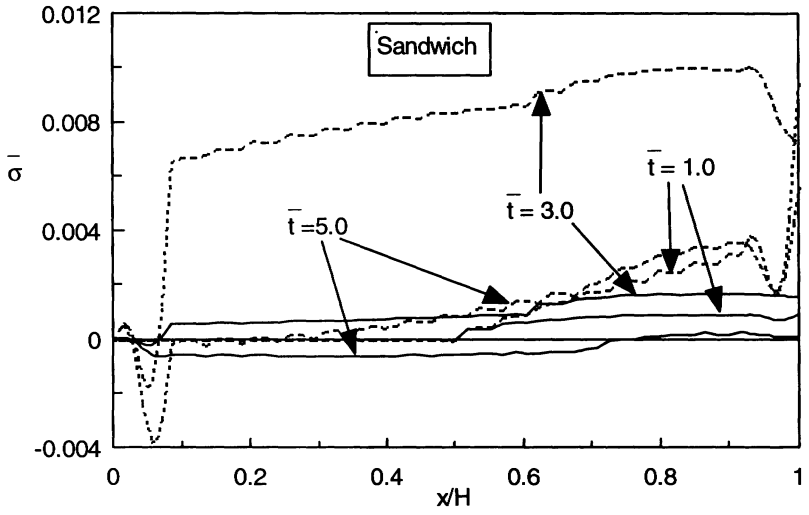

FIGURE 9 As in Fig. 8, but for $\bar{t}$ = 1.0, 3.0, and 5.0.

and the core layer is much softer than the two face layers. Hence, the right face layer can actually be treated as a single layer plate. It was noted earlier that the tensile stress in the plate can be produced by the reflection from the left surface of the plate. Therefore, there could be tensile stress produced in the left face layer, and the frequency of the stress sign changing should be very high because the face layer is very thin. On the other hand, due to the presence of the core layer, there are refractions of waves in the interface of the core layer and the right face layer. This results in only the partial left-going compressive wave reflected from the interface, and hence the tensile stress in the left face layer should be smaller than that for the single layer case. For the dry laminate the tensile stress in the left face layer could, however, be large as shown in Fig. 9.

Figure 10 shows the time history of the stress in the dry sandwich laminate. It is evident that a point near the right surface of the right face layer experiences a very high frequency oscillatory stress. This oscillatory stress is caused mainly at the reflections by the two surfaces of the left face layer. Figure 11 shows the time history of the stress in the sandwich wet laminate. From this figure, the oscillatory stress is also found at a point near to right surface of the right face layer.

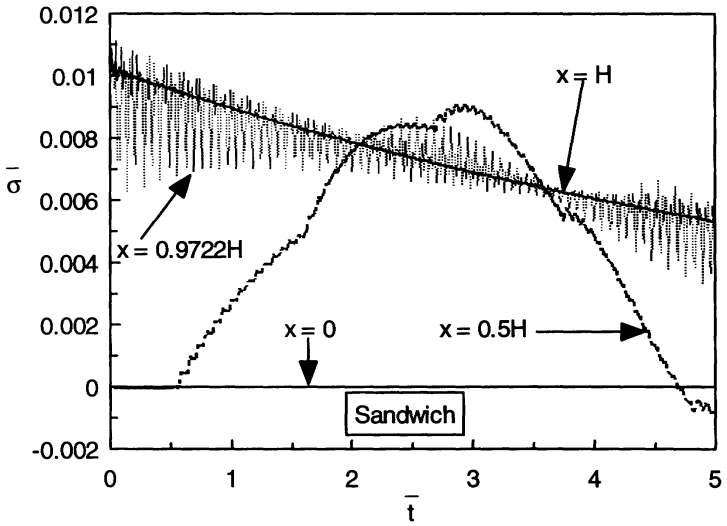

FIGURE 10 Stress history for the sandwich dry laminate subjected to an underwater explosion: TNT, 20 kg, D = 10 m.

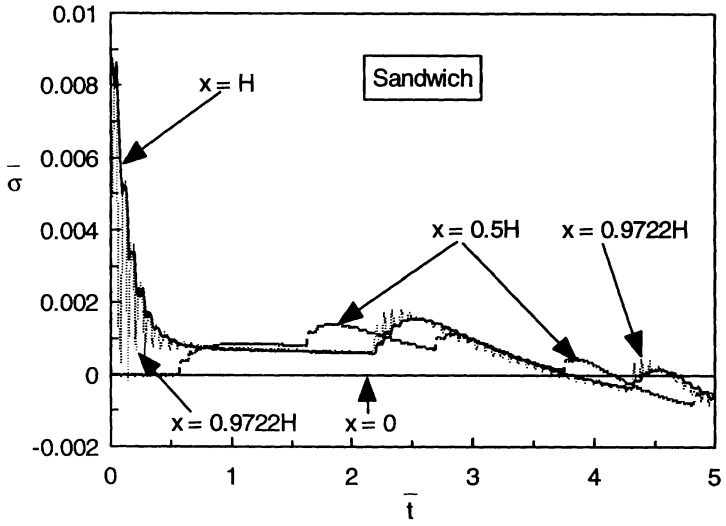

FIGURE 11 As in Fig. 10, but for the sandwich wet laminate.

In this case, however, the magnitude of the stress decays very fast and is much faster than for the steel wet plate (cf. Fig. 7). This is because the laminate is much softer than the steel plate. The displacement on the right surface of the sandwich laminate is, therefore, much greater than that in the steep plate, and a much lower shock pressure is taken by the sandwich laminate than that by the steel plate.

From Figs. 9 and 10 it can be seen again that the magnitudes of the compressive and tensile stress in the dry laminate is greater than that in the wet laminate. Therefore, the design is on the conservative side if the stresses are obtained by neglecting the plate–water interaction.

It should be mentioned that for the sandwich wet laminate, the pressure on the right laminate surface may become negative (see Fig. 11 for $\bar{t} > 4.8$). If the magnitude of the negative pressure is greater than the hydrostatic pressure, there would be cavitation, and the results are no longer valid or only valid for a structure in deep water where the hydrostatic pressure is great enough to prevent the cavitation.

The effects of the standoff distance D on the stress field in the laminate are also investigated. Figures 12 and 13 show the stress histories for the wet steel plate and sandwich laminate, respectively. The standoff distance D of the charge is 2 m. Comparisons of Figs. 7 and 12 and Figs. 11 and 13 suggest that there are no significant differences in the stress distributions for $D = 10$ and 2 m. However, due to the difference in the standoff distance, the magnitudes of the stress are significantly different.

CONCLUSIONS

In this article, a simple model was presented to analyze the stress fields in composite laminates. The model is used to compute the stress field in a steel and sandwich laminate subjected to underwater explosions. From the results, the following conclusions can be drawn.

- Any point in the laminate could experience compressive and tensile stress caused by the reflection of the stress wave generated by the pressure of the shock wave due to an underwater explosion. Therefore, the material of the laminate must withstand the compressive and tensile stresses.
- For the dry laminate the magnitude of the maximum tensile stress could be as high as the maximum compressive stress, the magnitude of which is as high as twice the peak magnitude of the shock pressure produced by the underwater explosion. For the wet laminate the magnitude of the maximum tensile stress is, however, smaller than the maximum compressive stress.
- Any point in the wet face layer of a sandwich

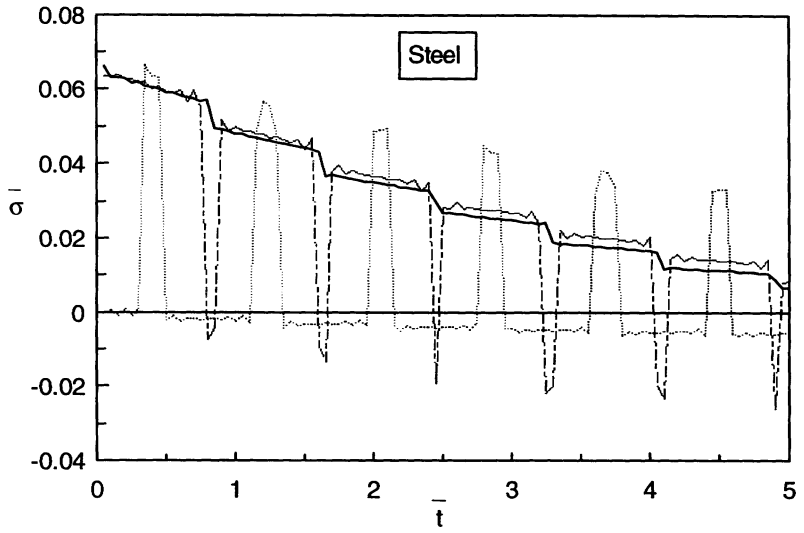

FIGURE 12 Stress history for the steel wet plate subjected to an underwater explosion: (——) $x = H$, (···) $x = 0.2H$, (---) $x = 0.9H$; TNT, 20 kg, $D = 2$ m).

laminate could experience a high frequency oscillatory stress.

- The magnitudes of the maximum compressive and tensile stress, computed by ignoring the laminate–water interaction and doubling the shock wave pressure, are greater than those obtained by considering the laminate–water interaction. Hence, a design based on the stresses computed by ignoring the laminate–water interaction is on the conservative side, but not economical.

It should be noted that the simple model presented here can be used to predict the stresses in the local region of a structure with many layers in the very early time just after the arrival of the shock wave. The global structural responses can be simulated by using existing finite element packages, such as the MSC/NASTRAN-USA code. The present study provides a tool for a quick check to see if the structure has been damaged locally or not, before running a large finite element package for the whole structure.

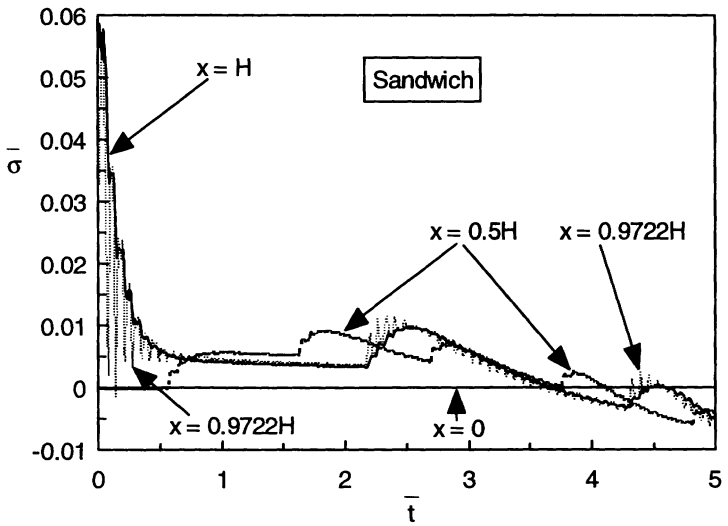

FIGURE 13 Stress history for the sandwich wet laminate subjected to an underwater explosion. TNT, 20 kg, $D = 2$ m).

REFERENCES

Geers, T. L., and Shin, Y. S., 1994, "Response of Marine Structures to Underwater Explosion, Part I: Theoretical Background," Lecture notes.

Green, A. K., 1982, "Assessment of Chopped Strand Mat GRP Lamination for the Construction of Damage Resistant Ship Hull Structures," *Composites*, Vol. 13, pp. 401–405.

Hall, D. J., 1989, "Examination of the Effects of Underwater Blasts on Sandwich Composite Structures," *Composite Structures*, Vol. 11, pp. 101–120.

Hall, D. J., and Robson, B. L., 1984, "A Review of the Design and Materials Evaluation Programme for the GRP/Foam Sandwich Composite Hull of the RAN Minehunter," *Composites*, Vol. 15, pp. 266–276.

Liu, G. R., and Achenbach, J. D., 1995, "Strip Element Method to Analyze Wave Scattering by Cracks in Anisotropic Laminated Plates," *ASME Journal of Applied Mechanics*, Vol. 62, pp. 607–613.

Liu, G. R., and Lam, K. Y. 1995, "An Exact Method for Analyzing Elastodynamic Response of Anisotropic Laminates to Line Loads," *Mechanics for Composite Materials and Structures*, Vol. 62, pp. 227–241.

Mouritz, A. P., Saunders, D. S., and Buckley, S., 1993, "The Damage and Failure of GRP Laminates by Underwater Explosion Shock Loading," *Proceedings of the 5th Australian Aeronautical Conference*, IE Australian, Part 2.

Trimming, M., 1978, "Marine Applications of Composites," in G. Piatti, *Advances in Composite Materials*, Applied Science Publishers, London, pp. 383–396.